Chemical Mechanism and Rate-Limiting Steps in the Reaction Catalyzed by *Streptococcus faecalis* NADH Peroxidase†

Vincent S. Stoll and John S. Blanchard*

Department of Biochemistry, Albert Einstein College of Medicine, 1300 Morris Park Avenue, Bronx, New York 10461

Received July 2, 1990; Revised Manuscript Received October 3, 1990

ABSTRACT: The pH dependence of the kinetic parameters V, V/K_{NADH}, and $V/K_{H_2O_2}$ has been determined for the flavoenzyme NADH peroxidase. Both V/K_{NADH} and $V/K_{H_2O_2}$ decrease as groups exhibiting pK's of 9.2 and 9.9, respectively, are deprotonated. The V profile decreases by a factor of 5 as a group exhibiting a pK of 7.2 is deprotonated. Primary deuterium kinetic isotope effects on NADH oxidation are observed on V only, and the magnitude of ^DV is independent of H_2O_2 concentration at pH 7.5. $^DV/K_{NADH}$ is pH independent and equal to 1.0 between pH 6 and pH 9.5, but ^DV is pH dependent, decreasing from a value of 7.2 at pH 5.5 to 1.9 at pH 9.5. The shape of the ^DV versus pH profile parallels that observed in the V profile and yields a similar pK of 6.6 for the group whose deprotonation decreases ^DV. Solvent kinetic isotope effects obtained with NADH or reduced nicotinamide hypoxanthine dinucleotide as the variable substrate are observed on V only, while equivalent solvent kinetic isotope effects on V and V/K are observed when H_2O_2 is used as the variable substrate. In all cases linear proton inventories are observed. Primary deuterium kinetic isotope effects on V for NADH oxidation decrease as the solvent isotopic composition is changed from H_2O to D_2O. These data are consistent with a change in the rate-limiting step from a step in the reductive half-reaction at low pH to a step in the oxidative half-reaction at high pH. Analysis of the multiple kinetic isotope effect data suggests that at high D_2O concentrations the rate of a single proton transfer step in the oxidative half-reaction is slowed. These data are used to propose a chemical mechanism involving the pH-dependent protonation of a flavin hydroxide anion, following flavin peroxide bond cleavage.

Flavoprotein reductases are members of a class of oxidoreductases, which include glutathione reductase (EC 1.6.4.2), lipoamide dehydrogenase (EC 1.8.1.4), and mercuric reductase (EC 1.16.1.1). Several of these enzymes have been investigated for over 20 years [reviewed in Williams (1976)]. In the case of glutathione reductase, three-dimensional structural information has been available for 10 years (Schulz et al., 1978), and the data have recently been refined to 1.5 Å (Karplus & Schulz, 1987). Both lipoamide dehydrogenase (Schierbeek et al., 1989) and mercuric reductase (Moore et al., 1989) have been crystallized, and crystallographic structural data will soon be available. Site-directed mutagenesis studies of glutathione reductase (Berry et al., 1989) and mercuric reductase (Schulz et al., 1985; Miller et al., 1990) have yielded information about nucleotide specificity, catalytic functionalities, and the chemical structures of short-lived intermediates. Despite their individual catalytic specificities, the flavoprotein reductases share extensive properties including quaternary structure, kinetic mechanism, stereochemistry of reduced pyridine nucleotide oxidation, spectral intermediates, and primary sequence of the active site peptide containing the redox-active disulfide responsible for reversible electron storage.

NADH peroxidase (EC 1.11.1.1) shares many of these same properties (Dolin, 1975; Poole & Claiborne, 1986; Stoll & Blanchard, 1988) with the important exception that the enzyme contains a single cysteine residue per monomer (Poole & Claiborne, 1988). This is a remarkable finding considering that the chemistry occuring in the oxidative half-reactions of the known flavoprotein reductases relies on the presence of the disulfide/dithiol moiety in the conserved active site peptide. To reconcile this finding with the required ability of NADH peroxidase to reversible store two electrons, it has been proposed that the single cysteine residue is present as a sulfenic acid (-SOH) in the oxidized form of the enzyme and is reduced to the thiol by NADH.[1] This unusual oxidation state for sulfur has precedent in the literature of the selenium-containing glutathione peroxidase, where the selenic acid (-SeOH) has been proposed as an intermediate in the decomposition of hydrogen peroxide (Flohe et al., 1972).

NADH peroxidase from *Streptococcus faecalis* 10C1 has been crystallized in a form that diffracts to high resolution and maintains its catalytic competence in the crystal (Schiering et al., 1989). The purpose of this study is to define the rate-limiting steps in the reaction and the chemistry which may be involved in these steps. The combination of pH and kinetic isotope effect studies has yielded information on these steps and has allowed us to propose a chemical mechanism which incorporates the role of a single redox-active cysteine residue.

Materials and Methods

NADH peroxidase from *S. faecalis* was purchased from Sigma and was greater than 95% pure by SDS-polyacrylamide gel electrophoresis and Coomassie staining. Glucose-6-

† This work was supported by Grant GM33449 awarded by the NIH and the Sinsheimer Scholar Foundation.

* Author to whom correspondence should be addressed.

[1] Abbreviations: FPLC, fast protein liquid chromatography; NADH, reduced β-nicotinamide adenine dinucleotide; NHDH, reduced β-nicotinamide hypoxanthine dinucleotide; thioNADH, reduced β-thionicotinamide adenine dinucleotide; 3-APADH, reduced β-3-acetylpyridine adenine dinucleotide; 3-APHDH, reduced β-3-acetylpyridine hypoxanthine dinucleotide; NGDH, reduced β-nicotinamide guanine dinucleotide; TEA-HCl, triethanolamine hydrochloride; Bis-Tris, [bis(2-hydroxyethyl)amino]tris(hydroxymethyl)methane; MES, 2-(*N*-morpholino)ethanesulfonic acid; BES, *N*,*N*-bis(2-hydroxyethyl)-2-aminoethanesulfonic acid; PIPES, 1,4-piperazinediethanesulfonic acid; HEPES, *N*-(2-hydroxyethyl)piperazine-*N*'-2-ethanesulfonic acid; TAPS, 3-[[tris(hydroxymethyl)methyl]amino]propanesulfonic acid; CHES, 2-(cyclohexylamino)ethanesulfonic acid.

0006-2960/91/0430-942$02.50/0

phosphate dehydrogenase from *Leuconostoc mesenteroides* (type XXIV) was from Sigma. All pyridine nucleotides were purchased from Sigma. D-[1-^{2}H]Glucose (≥98 atom % excess ^{2}H) was purchased from Amersham. D-[1-^{3}H]Glucose was purchased from Amersham. The [4-^{3}H]NAD and [*adenine*-^{14}C]NAD were purchased from New England Nuclear. All other chemicals and reagents were of the highest purity commericially available.

Preparation of Reduced Pyridine Nucleotides. All (4*S*)-4-^{1}H- and (4*S*)-4-^{2}H-labeled reduced pyridine nucleotides were prepared and purified as previously described (Stoll & Blanchard, 1988). Peak fractions were diluted 1:100 into 10 mM TEA buffer, pH 7.8, and their spectra were recorded on a Cary 219 recording spectrophotometer. Fractions which had acceptable absorbance ratios (e.g., $A_{260}/A_{340} \leq 2.3$ for NADH) were pooled. These solutions were calibrated enzymatically with NADH peroxidase and an excess of hydrogen peroxide.

Kinetic Procedures. NADH peroxidase reaction rates were measured spectrophotometrically by monitoring the oxidation of NADH at 340 nm with $\epsilon = 6220\ M^{-1}\ cm^{-1}$ on a Gilford 260 spectrophotometer equipped with thermospacers attached to a constant-temperature circulating water bath maintained at 25 °C. Reactions were initiated by the addition of a small volume (≤20 μL) of cold enzyme solution to the temperature-equilibrated cuvette.

pH Profiles. The following buffers (300 mM) were prepared by titrating their acid forms, dissolved in water, to the desired pH with 2 N KOH and were used at 100 mM final concentrations at the stated pHs to allow for overlap: Bis-Tris (5.8–6.9), MES (6.0–6.6), BES (6.2–7.2), PIPES (6.6–7.4), HEPES (7.0–8.2), TAPS (8.1–9.0), and CHES (8.9–10.5). pH values were measured with a Radiometer PHM84 pH meter equipped with a combined microelectrode. The kinetic parameters V and V/K for the variable substrate were determined at each pH, and their log values were plotted against pH, determined by insertion of a combined microelectrode into the cuvette after the initial velocity assays were carried out.

Solvent Kinetic Isotope Effects and Preparation of Isotopic Solvents. Buffers were prepared by titrating H_2O or D_2O solutions containing 300 mM HEPES to pH or pD (pH meter reading + 0.4) 7.5 with KOH in H_2O or D_2O, respectively. Sodium acetate was dissolved in a small volume of D_2O, after which the solvent was removed by rotary evaporation. The solid was then redissolved in D_2O.

Reaction mixtures containing NADH or NHDH, H_2O_2, and the desired mole fraction of H_2O and D_2O buffer solutions were prepared in 3-mL cuvettes. Initial velocities were measured at various mole fractions of D_2O with varying NHDH or H_2O_2 concentrations, in the presence of a saturating concentration of the other substrate. The kinetic parameters V and V/K were determined, and calculated values of V and V/K were plotted against mole fraction of D_2O. The resulting proton inventories were used to determine the number of protons transferred and the solvent kinetic isotope effects on V (^{D_2O}V) or on V/K ($^{D_2O}V/K$).

pH Dependence of the Primary Deuterium Kinetic Isotope Effects. Protio and deutero nucleotides were prepared as described above. Initial velocities were measured at varying nucleotide concentrations for both protio and deutero nucleotides at fixed concentrations of H_2O_2 determined to be saturating at pH values between 4.8 and 9.8. The reciprocal initial velocities were plotted against reciprocal substrate concentrations, and the data were fitted to eq 4 (below).

Data Analysis. Reciprocal initial rates were plotted against reciprocal substrate concentrations, and the data were fitted to the appropriate equations with the Fortran programs of Cleland (1979). Individual saturation curves were fitted to eq 1, where A is the variable substrate concentration. Data for pH profiles that showed a decrease in log (V/K) with a slope of −1 as the pH was increased were fitted to eq 2. In eq 2, y is the parameter whose pH dependence is being determined (V/K_{NADH} or $V/K_{H_2O_2}$), and C is the pH-independent value of y at low pH. The data for the pH profiles of V and ^DV were fitted to eq 3, where y is the parameter whose pH dependence is being determined, K is the dissociation constant for the group whose protonation increases V and ^DV, A is the pH-independent value of V or ^DV at low pH values, and B is the difference in the value of y at low and high pH values. Isotope effects on the oxidation of reduced pyridine nucleotides were calculated from eq 4, where A is the NADH concentration, F_i is the fraction of deuterium label in deuterated nucleotide (=1.0), and E_V is the isotope effect minus 1 for V. The initial velocities obtained by varying the concentration of either NHDH or H_2O_2 at different mole fractions of D_2O were fitted to eq 4 (using NHDH as the variable substrate) or eq 5 (using H_2O_2 as the variable substrate), which assumes solvent kinetic isotope effects on V only and on both V and V/K, respectively. In eqs 4 ands 5, A is the variable substrate concentration, F_1 is the mole fraction of D_2O, and $E_{V/K}$ are the solvent kinetic isotope effects minus 1 for V and V/K, respectively.

$$v = VA/(K + A) \quad (1)$$

$$\log y = \log [C/(1 + K_1/[H^+])] \quad (2)$$

$$y = A + B/(1 + [H^+]/K) \quad (3)$$

$$v = VA/[K + A(1.0 + F_iE_V)] \quad (4)$$

$$v = VA/[K(1.0 + F_iE_{V/K}) + A(1.0 + F_iE_V)] \quad (5)$$

Table I: Dependence of the Primary Deuterium Kinetic Isotope Effect on the Concentration of Hydrogen Peroxide[a]

$[H_2O_2]$ (μM)	^DV[b]
100	2.59 ± 0.27
50	2.45 ± 0.17
33	2.12 ± 0.19
20	2.25 ± 0.24

[a] All data were obtained in 100 mM HEPES buffer, pH 7.8 at 25 °C. [b] Primary deuterium kinetic isotope effects were determined by varying the concentration of [4(*S*)-^{1}H]- and [4(*S*)-^{2}H]NADH, and the data were fit to eq 4.

Results

Effect of pH on the Kinetic Parameters. The pH profiles shown in Figure 1 (top and bottom) were obtained when NADH was varied at a saturating concentration of H_2O_2 (over 50 $K_{mH_2O_2}$ at all pHs) at pH values between 5.2 and 10.5. The maximum velocity is highest at low pH and decreases 5-fold to a lower value at high pH. A pK value of 7.20 ± 0.17 was determined from these data. The V/K_{NADH} profile shows a decrease in activity at high pH as a group with a pK value of 9.33 ± 0.15 is deprotonated.

When H_2O_2 was the varied substrate at a fixed, saturating concentration of NADH (over 40K_{mNADH} at all pH values) from pH 5.8 to 10.6 and the data were fitted to eq 1, the $V/K_{H_2O_2}$ pH profile shown in Figure 1 (middle) was obtained. The $V/K_{H_2O_2}$ decreases at high pH as a group with a pK of 9.92 ± 0.09 is deprotonated.

pH Dependence of the Primary Deuterium Kinetic Isotope Effects. The effect of hydrogen peroxide concentration on the primary deuterium kinetic isotope effects were determined at

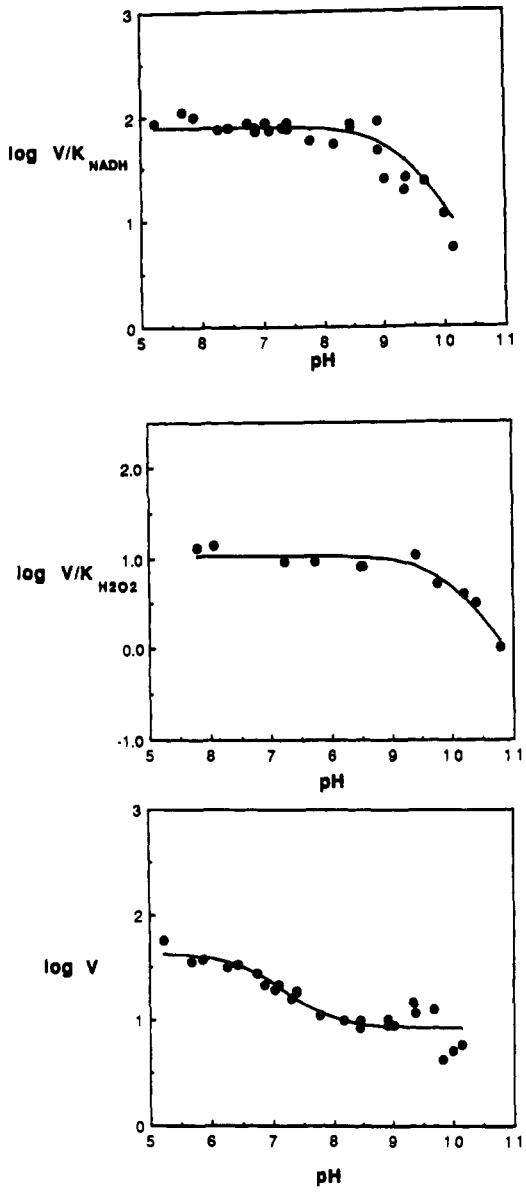

FIGURE 1: Effect of pH on kinetic parameters V, V/K_{NADH}, and $V/K_{H_2O_2}$. The individual experimental points are fits of the data to eq 1, and the smooth curves for V/K_{NADH} pH and $V/K_{H_2O_2}$ pH profiles are fits of the data to eq 2. The V pH profile was fit to eq 3. The V/K_{NADH} profile (top) decreases as a single enzymic group with a pK_a of 9.33 ± 0.15 is deprotonated. The $V/K_{H_2O_2}$ profile (middle) decreases as a single enzymic group with a pK_a of 9.92 ± 0.09 is deprotonated. The V profile (bottom) shows an increase in activity at low pH, as a group exhibiting a pK of 7.20 ± 0.17 is protonated.

pH 7.8 (Table I). There was no statistically significant change in the observed isotope effects. The primary deuterium kinetic isotope effects on V and V/K were determined over the pH range from 9.8 to 4.8. As the pH decreases from pH 9.8 to pH 4.8, ^DV increases (Figure 2). A pK values of 6.62 ± 0.15 was determined for the group whose protonation increases ^DV from these data with eq 3. There is no significant change in $^DV/K_{NADH}$ at pH values between 9.8 and 6.7; however, the $^DV/K$ appears to become slightly greater than unity (1.2–1.5) at pH values below 6.7.

Solvent Kinetic Isotope Effects and Proton Inventories. The low K_m value for NADH ($K_{m,NADH}$ = 2.5 μM) made it difficult to measure initial velocities at high molar fractions of D_2O, so the alternative substrate, NHDH ($K_{m,NHDH}$ = 25 μM; V = 98% that of NADH; Stoll & Blanchard, 1988), was used to determine D_2O solvent kinetic isotope effect on the individual kinetic parameters.

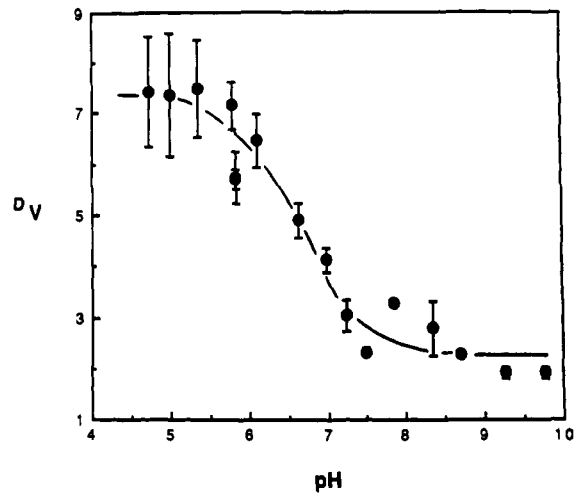

FIGURE 2: Effect of pH on the primary deuterium kinetic isotope effects on V. Individual points are the fits of the data to eq 4, and the smooth curve through the data is a fit of the data to eq 3. The magnitude of the ^DV profile increases at low pH, as a group with a pK of 6.62 ± 0.15 is protonated.

Table II: Dependence of the Primary Deuterium Kinetic Isotope Effect on D_2O Concentration[a]

% D_2O	$^DV^b$
0	2.04 ± 0.02
28	2.19 ± 0.05
56	1.71 ± 0.07
88	1.41 ± 0.02

[a] All data were obtained in 100 mM TAPS buffer, pH 8.1, containing 3 mM H_2O_2 at 25 °C. [b] Primary deuterium kinetic isotope effects were determined by varying the concentration of [4(*S*)-^{1}H]- and [4-(*S*)-^{2}H]NADH, and the data were fit to eq 4.

When NHDH was the variable substrate at a fixed saturating concentration of H_2O_2, the data shown in Figure 3A were obtained. When values of V_{NHDH} determined at each mole fraction of D_2O were plotted versus mole fraction D_2O, a linear proton inventory was obtained, and a ^{D_2O}V solvent kinetic isotope effect of 2.7 ± 0.2 was observed. When H_2O_2 was varied at a fixed saturating concentration of NADH, at various mole fractions of D_2O, intersecting reciprocal plots were obtained as shown in Figure 3B. When fitted values for V and $V/K_{H_2O_2}$ were plotted versus mole fraction of D_2O, proton inventories were obtained (see insets) which yielded identical values for ^{D_2O}V and $^{D_2O}V/K_{H_2O_2}$ of 2.4 ± 0.1. The solid lines in the insets represent fits to the Gross–Butler equation for a monoprotonic transition state with Φ^T = 0.413, while the dashed lines represent fits for a diprotonic transition state with Φ^T = 0.637.

The effect of D_2O on the primary deuterium kinetic isotope effect was performed by varying either NADH or [(4*S*)-4-^{2}H]NADH at various mole fractions of D_2O. The data shown in Table II were obtained. The primary deuterium kinetic isotope effect on V decreased from a value of 2.04 ± 0.02 to a value of 1.41 ± 0.02 as the mole fraction of D_2O was increased.

Discussion

pH Profile of the Kinetic Parameters. The V/K pH profile for NADH decreases at high pH as a group with a pK value of 9.33 ± 0.15 is deprotonated. The V/K_{NADH} pH profile depends on the ionization behavior of groups on either free oxidized enzyme or NADH which affect either catalysis or the interaction of the enzyme and NADH. NADH does not have any titratable groups in this range, and it can be con-

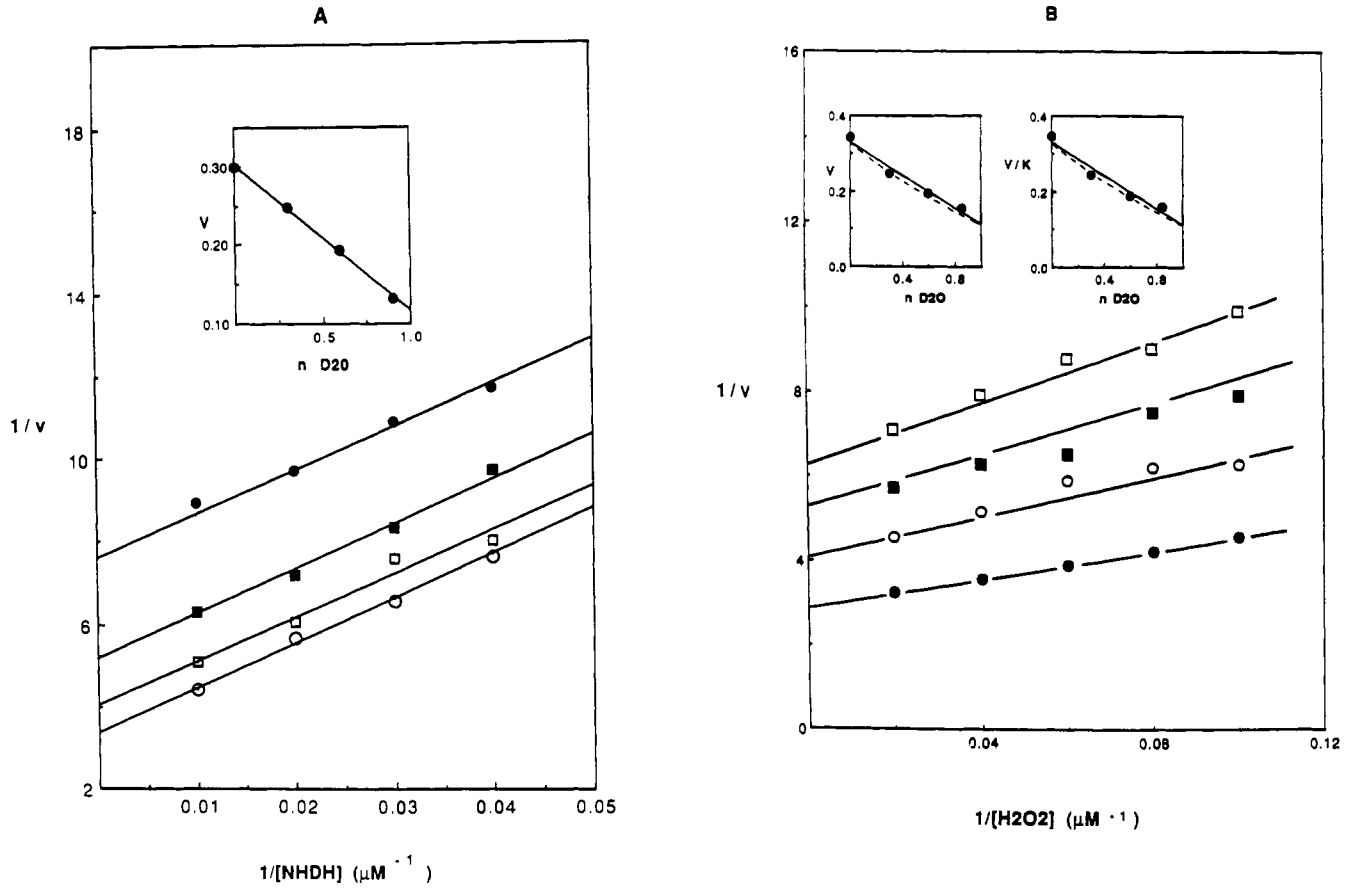

FIGURE 3: (A) Solvent kinetic isotope effects using NHDH as the variable substrate. Double-reciprocal plot of the initial velocity using NHDH as the variable substrate and a fixed, saturating concentration of H_2O_2 (1 mM), at various mole fractions of D_2O. The lines through the data points are the fit to eq 4, where solvent kinetic isotope effects are manifested on V only, and yield a value for ^{D_2O}V of 2.70 ± 0.14. The inset shows the replot of V versus $\eta(D_2O)$. (B) Solvent kinetic isotope effects using H_2O_2 as the variable substrate. Double-reciprocal plot of the initial velocity using H_2O_2 as the variable substrate and a fixed, saturating concentration of NADH (100 μM), at various mole fractions of D_2O. The lines through the data points are the fit to eq 5, where equivalent solvent kinetic isotope effects on V and V/K are manifested, with $^{D_2O}V = {}^{D_2O}V/K_{H_2O_2} = 2.4 \pm 0.1$. The insets show the replots of V and $V/K_{H_2O_2}$ versus $\eta(D_2O)$, where the solid lines represent fits for a monoprotonic transition state and where the dashed lines represent fits for a diprotonic transition state.

cluded that the deprotonation of a group on the free enzyme is reflected. In human erythrocyte glutathione reductase a group exhibiting a pK value of 9.8, whose deprotonation decreases V/K for several nucleotide substrates and increases the K_i of competitive inhibitors, has been attributed to an arginine residue adjacent to the adenine ring in the nucleotide binding domain (Wong & Blanchard, 1989). The pK value that we see for NADH peroxidase may similarly be attributable to a group in the adenine ring portion of the nucleotide binding region of this enzyme. This group may alternatively be ascribed to the acid which protonates hydroxide ion formed from cleavage of the S–O bond of the sulfenic acid or to the sulfenic acid itself. Sulfenic acid pK's have been reported in the pH range of 7–9 (Kice, 1980), and deprotonation of either of these groups would be expected to slow the rate of catalysis in the reductive half-reaction. No evidence for this was obtained by examination of the V pH profile (see below) or from the determination of kinetic isotope effects at high pH.

The V/K profile for H_2O_2 decreases at high pH as a group exhibiting a pK value of 9.92 ± 0.09 is deprotonated. This pK is not due to the ionization of H_2O_2 since its pK_a value is 11.75 (Manly, 1962), and therefore, this pK must be due to the deprotonation of a group on the two-electron-reduced enzyme. It is unlikely that this pK can be assigned to the redox-active cysteine residue, as the pK of this group has been reported to be 5.4 from spectroscopic titrations (Poole & Claiborne, 1986). The identity of this group must await further experimentation.

The V pH profile for NADH peroxidase is determined by the ionization behavior of enzymic groups involved in catalysis and does show a slight decrease in activity above pH 7; however, this decrease reaches a plateau and does not attain a slope of −1. The data yield a pK value of 7.20 ± 0.17. This pK is likely to be either an enzymic group involved in the protonation of the proposed sulfenic acid in the reductive half-reaction and/or protonation events involved in bond cleavage of a flavin-bound peroxide. From these data it can be concluded that deprotonation of this enzymic group decreases but does not abolish activity. To distinguish between these two possibilities, the pH dependence of the primary deuterium kinetic isotope effects was analyzed as a function of pH.

pH Dependence of the Primary Deuterium Kinetic Isotope Effects. The primary deuterium kinetic isotope effect is independent of the concentration of H_2O_2 (Table I). Varying the substrate concentration for the non-isotope-dependent half-reaction of a ping-pong kinetic mechanism should produce no effect, as shown previously with glutathione reductase (Vanoni et al., 1990). All subsequent primary deuterium kinetic isotope effects were determined at a saturating concentration of hydrogen peroxide.

The primary deuterium kinetic isotope effects were measured over the pH range between 4.74 and 9.77. As shown in Figure 2, ^{D}V exhibits a pH dependence similar to that observed on V, and fitting the ^{D}V values to eq 3 yields a pK value of 6.62 ± 0.15 for a group whose deprotonation decreases ^{D}V. This value is close to that determined from the pH de-

pendence of V and likely reflects the same group.

To determine which steps in the overall reaction mechanism are affected by pH and might contribute to the pH dependence of the kinetic isotope effect, a ping-pong reaction mechanism was modeled. In the proposed mechanism, the assumption is made that peroxo bond cleavage, k_9, is irreversible due to the large loss in free energy accompanying reduction of H_2O_2 to water. Using the net rate constant method of Cleland (1975), eqs 6–10 can be derived for the mechanism below, where k_3* is the isotopically sensitive step when [(4*S*)-4-^{2}H]NADH is used as substrate:

$$E_{ox} + NADH \underset{k_2}{\overset{k_1}{\rightleftharpoons}} E_{ox}\cdot NADH \underset{k_4}{\overset{k_3^*}{\rightleftharpoons}} E_{red}\cdot NAD^+ \xrightarrow{k_5} E_{red} + NAD^+$$

$$E_{red} + H_2O_2 \underset{k_8}{\overset{k_7}{\rightleftharpoons}} E_{red}\cdot H_2O_2 \xrightarrow{k_9} E_{ox}\cdot 2H_2O \xrightarrow{k_{11}} E_{ox} + 2H_2O$$

$$^DV/K_{NADH} = \frac{^Dk_3 + c_f + c_r{}^DK_{eq}}{1.0 + c_f + c_r} \quad (6)$$

$$^DV = \frac{^Dk_3 + c_{vf} + c_r{}^DK_{eq}}{1.0 + c_{vf} + c_r} \quad (7)$$

where

$$c_f = k_3/k_2 \quad (8)$$

$$c_r = k_r/k_5 \quad (9)$$

and

$$c_{vf} = k_3/k_5 + k_3/k_9 + k_3/k_{11} \quad (10)$$

$$^DK_{eq} = k_{3H}k_{4D}/k_{3D}k_{4H} \quad (11)$$

The commitment factors, c_f, c_r, and c_{vf}, are rate constant ratios whose magnitude will affect the size of an observed isotope effect relative to the intrinsic isotope effect, $^Dk_3$. A $^DV/K_{NADH}$ of unity at pH values between 6 and 10.5 suggests that NADH dissociated from the E·NADH binary complex more slowly than it transfers its hydride ion to FAD, resulting in a large value of c_f. The product, NAD^+, has been shown to bind weakly to the reduced form of the enzyme (Stoll & Blanchard, 1988), suggesting that the reverse commitment factor, k_4/k_5, is also small and will not contribute significantly to either $^DV/K$ or ^DV. Thus, the change observed in ^DV as the pH is varied can be interpreted as a change in c_{vf}. At high pH, c_{vf} must be large relative to its value at low pH. The equation that defines c_{vf} is composed of the sum of the ratios of k_3 to k_5, k_9, and k_{11}, any of which could, potentially, be pH dependent and result in the observed change in the magnitude of ^DV with pH. As mentioned above it has been shown that NAD^+ is a poor product inhibitor and dissociates rapidly, which suggests that k_5 will be fast relative to k_3. It is also unlikely that H_2O dissociates slowly from the enzyme, and both k_3/k_5 and k_3/k_{11} will likely be near zero. The expression for c_{vf} is then k_3/k_9, or the ratio of the catalytic rate constants for EH_2 formation and its breakdown. Thus at high pH (e.g., pH 9.0) the rate of enzyme reduction, k_3, is faster than that of enzyme oxidation, k_9, and ^DV will be smaller than $^Dk_3$. As the pH decreases, either k_3 slows relative to k_9 or k_9 increases relative to k_3. The overall maximum velocity of the reaction increases with decreasing pH, making the latter interpretation more plausible. The results suggest the presence of an enzymic group that, when protonated, enhances the rate of the oxidative half-reaction. Deprotonation of this group does not abolish activity but does increase the value of c_{vf} by slowing the catalytic rate of the oxidative half-reaction. Conclusions similar to our own have been obtained from an analysis of the pH dependence of the maximum velocity and the primary deuterium kinetic isotope effect on the maximum velocity of the ping-pong kinetic mechanism catalyzed by the flavoprotein dihydroorotate dehydrogenase from bovine liver (Hines & Johnston, 1989).

Proton Inventories and D_2O Solvent Kinetic Isotope Effects. The analysis of the pH dependence of the primary deuterium kinetic isotope effects suggests that the rate of the oxidative half-reaction and the overall reaction depends on the protonation state of an enzymic group involved in the oxidative half-reaction. Any plausible chemical mechanism for the oxidative half-reaction must include proton transfer step(s), and the solvent kinetic isotope effect studies performed confirm and extend these observations. With NADH as the variable substrate, a solvent kinetic isotope effect on V only of 2.7 was observed at pH 7.55, with no statistically significant effect on V/K. The replot of V versus mole fraction of D_2O was linear (Figure 3A), confirming that a single proton transfer was responsible for the isotope effect. No effect of solvent isotopic composition on V/K for NHDH was observed, suggesting that the proton transfer step is not a rate-limiting event in the reductive half-reaction.

A different pattern was observed when H_2O_2 was used as the variable substrate at various fixed concentrations of D_2O. Identical solvent kinetic isotope effects of 2.4 were observed on both V and V/K. Proton inventories appeared linear in both cases, indicating that the same proton transfer step was again responsible for the observed isotope effect. The equal magnitudes of the solvent kinetic isotope effects observed on both V and $V/K_{H_2O_2}$ suggest that the proton transfer step is localized in the oxidative half-reaction.

Multiple Isotope Effects. The pH dependence of the primary deuterium kinetic isotope effect on NADH oxidation suggested that the protonation state of a catalytic group on the enzyme could change the ratio of the two catalytic rate constants, k_3 and k_9. This is proposed to be a specific effect on k_9, with the rate of the oxidative half-reaction increasing with decreasing pH. The analysis of the solvent kinetic isotope effect data also suggests that a step in the oxidative half-reaction (k_9) is slowed by a factor of ≈2.4 in 100% D_2O. If the only term in eq 10 that contributes to c_{vf} is the ratio k_3/k_9, then ^DV should change as the isotopic composition of the solvent changes. Specifically, k_{9,H_2O} will be replaced in the expression by k_{9,D_2O}, which is 2.4 times smaller, causing c_{vf} to increase in D_2O, resulting in a decrease in ^DV with increasing concentrations of D_2O. As shown in Table II, ^DV decreases from a value of 2.0 ± 0.1 to a value of 1.4 ± 0.1 in 0 and 88% D_2O, respectively.[2] If k_3/k_5 or k_3/k_{11} were contributing to c_{vf}, no dependence of ^DV on solvent isotopic composition would be expected.

Chemical Mechanism. A common characteristic of the flavoprotein reductase family is the presence of a redox-active disulfide and the formation of the charge transfer complex upon two-electron reduction. NADH peroxidase is an unusual variant since the enzyme contains only one cysteine residue per monomer and contains no intersubunit disulfide bonds

[2] Using eq 7, where $^Dk_3$ must be equal to or greater than 7.5, we can calculate the expected decrease in ^DV at pH 7.8, if k_{9,D_2O} is 2.4 times slower than k_{9,H_2O}. The value of $k_3/k_{9,H_2O}$ is 4.4, while the corresponding value of $k_3/k_{9,D_2O}$ is 10.6. If this were the only term in c_{vf}, ^DV can be calculated to go from 2.2 to 1.6, in reasonable agreement with our experimentally determined values.

Scheme I: Proposed Chemical Mechanism for NADH Peroxidase

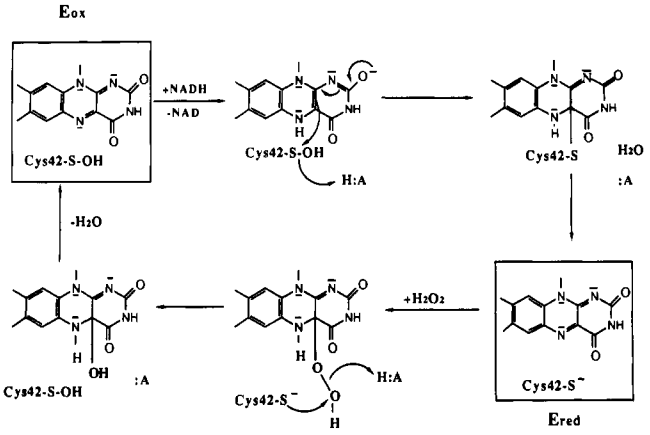

(Poole & Claiborne, 1989a). The spectrum of the enzyme is characterized by the appearance of a long-wavelength band centered at 525 nm upon reduction with NADH (Dolin, 1975; Poole & Claiborne, 1986), analogous to those observed in the other flavoprotein reductases (Williams, 1976). Early suggestions that this long-wavelength band was due to a thiolate–flavin charge transfer complex have been confirmed. In the case of glutathione reductase, X-ray crystallographic analysis has demonstrated the close proximity (3.48 Å) of the thiol of cysteine 63 to the C_{4a} position of the isoalloxazine ring (Karplus & Schulz, 1987). For mercuric reductase, conversion of cysteine 140 to a serine residue abolished the long-wavelength absorbance (Schulz et al., 1985). In the case of NADH peroxidase, the chemical identity of the second redox active center in the oxidized enzyme has reasonably been ascribed to a sulfenic acid, which is reduced to the thiol upon addition of NADH (Poole & Claiborne, 1989b). On the basis of this information and the data presented here, the chemical mechanism shown in Scheme I is proposed.

In the oxidized enzyme, E_{ox}, Cys42 is present at the oxidation level of a sulfenic acid. Binding of NADH and subsequent hydride transfer result in the formation of the two-electron-reduced enzyme, E_{red}, with the spectroscopically identified charge transfer complex. NAD^+ is released, and evidence has been presented that under steady-state conditions a second molecule of NADH binds to form EH_2·NADH (Stoll & Blanchard, 1988). By analogy to glutathione reductase, there must be a number of individual chemical steps between E_{ox} and E_{red}, the first being hydride transfer from NADH to FAD. Transient flavin reduction to form $FADH_2$ or $FADH^-$ (the C_2 enolate)[3] has never been observed for any native flavoprotein reductase, even by rapid kinetic methods. However, recent mutagenesis studies on mercuric reductase have allowed several intermediates in the reductive half-reaction to be characterized (Miller et al., 1990), particularly the enolate form of $FADH^-$. Additional support for the transient formation of the enolate comes from glutathione reductase, where a long α-helix is positioned above the C_2 oxygen of the isoalloxazine ring and whose dipole moment is appropriate for the stabilization of developing negative charge at C_2 (Schulz et al., 1982). Flavin reduction is quickly followed by electron transfer to the sulfenic acid, releasing H_2O and forming a C_{4a} thiol adduct. This covalent complex is electronically equivalent to a noncovalent thiolate–FAD complex, whose spectroscopic signature is the long-wavelength charge transfer band.

In the oxidative half-reaction, it has been proposed that hydrogen peroxide binds covalently to the C_{4a} position of the flavin, followed by nucleophilic attack by the thiolate anion (of Cys42) on the terminal oxygen atom of the flavin peroxide (Stoll & Blanchard, 1988). In the oxidation of *p*-mercaptobenzoate by *p*-hydroxybenzoate hydroxylase, a similar nucleophilic attack by a substrate-derived thiol on a flavin peroxide intermediate has been proposed to yield a sulfenic acid and the flavin hydroxide (Entsch et al., 1976). Peroxo bond cleavage in the oxidative half-reaction of NADH peroxidase would be facilitated by protonation of the flavin-proximate oxygen by an enzymic acid. By this mechanism, the sulfenic acid is regenerated, and water is formed from the decomposition of the 4a-hydroxyflavin.

In this mechanism, two proton transfers are drawn; one in the reductive half-reaction involving protonation of the sulfenic acid and the other in the reductive half-reaction involving peroxo bond cleavage. From the pH dependence of V, it can be concluded that neither of these proton transfers is essential for activity; however, protonation of an enzymic group permits a proton transfer to occur, which increases the rates of the overall reaction. No evidence for the titration of the Cys42 thiolate anion was observed in these experiments. The reported pK of this group of 5.4 (Poole & Claiborne, 1986) was determined by titrating the two-electron-reduced enyme in the absence of reduced pyridine nucleotide, while these studies have been performed under conditions where the two-electron-reduced enzyme would also contain a bound NADH (i.e., E_{red}–NADH versus E_{red}). It is likely that the presence of bound NADH would perturb the pK of the thiolate anion, and our data suggest that the pK of the Cys42 thiol is reduced by the binding of NADH. The pH dependence of the primary deuterium kinetic isotope effects and the solvent kinetic isotope effects requires that the titration of an enzymic group observed in the V pH profile affects the rate of chemical events in the oxidative half-reaction. The oxidative half-reaction is rate limiting at neutral and high pH, while at low pH the rate of the oxidative half-reaction increases so that hydride transfer from NADH to flavin is partially or fully rate determing as evidenced by the magnitude of the primary deuterium kinetic isotope effect. The data presented here suggest the protonation state of an enzymic acid can modulate the rate of the oxidative half-reaction by facilitating peroxo bond cleavage. When protonated, the products of peroxo bond cleavage are the sulfenic acid and the flavin 4a-hydroxide; when unprotonated, the products are the sulfenic acid and the flavin hydroxide anion. The pK value for the free flavin 4a-hydroxide in solution has been reported to be between 9.1 and 9.5 (Bruice, 1982), and the enzyme presumably can further stabilize this intermediate. The chemical identity of this acid is being investigated by X-ray crystallography, since the enzyme has been crystallized (Schiering et al., 1989) and is catalytically active in the crystal.

[3] Reduced $FADH_2$ exhibits a pK of 6.25 in solution (Clark, 1972), and both the N_1 anion and the C_2 enolate tautomer are considered the likely chemical species of $FADH^-$.

References

Bruice, T. C. (1982) in *Flavins and Flavoproteins* (Massey, V., & Williams, C. H., Jr., Eds.) pp 265–277, Elsevier, New York.

Clark, W. M. (1972) *Oxidation Reduction Potentials of Organic Systems*, p 129, R. E. Creiger, Huntington, NY.

Cleland, W. W. (1975) *Biochemistry 14*, 3220.

Cleland, W. W. (1979) *Methods Enzymol. 63*, 103.

Dolin, M. I. (1975) *J. Biol. Chem. 250*, 310.

Entsch, B., Ballou, D. P., Husain, M., & Massey, V. (1976) *J. Biol. Chem. 245*, 7367.

Flohe, L., Loschen, G., Gunzler, W. A., & Eichele, E. (1972) *Hoppe-Seyler's Z. Physiol. Chem. 353*, 987.
Hines, V., & Johnston, M. (1989) *Biochemistry 28*, 1227.
Karplus, P. A., & Schulz, G. E. (1987) *J. Mol. Biol. 195*, 701.
Kice, J. L. (1980) *Adv. Phys. Org. Chem. 17*, 65.
Manly, T. D. (1962) *Chem. Ind.*, 12.
Miller, S. M., Massay, V., Ballou, D., Williams, C. H., Jr., Distefano, M. D., Moore, M. J., & Walsh, C. T. (1990) *Biochemistry 29*, 2831.
Moore, M. J., Distefano, M. D., Walsh, C. T., Schiering, N., & Pai, E. F. (1989) *J. Biol. Chem. 264*, 14386.
Poole, L. B., & Claiborne, A. (1986) *J. Biol. Chem. 261*, 14525.
Poole, L. B., & Claiborne, A. (1988) *Biochem. Biophys. Res. Commun. 153*, 261.
Poole, L. B., & Claiborne, A. (1989a) *J. Biol. Chem. 264*, 12322.
Poole, L. B., & Claiborne, A. (1989b) *J. Biol. Chem. 264*, 12330.
Schierbeek, A. J., Swarte, M. B., Dijkstra, B. W., Vriend, G., Read, R. J., Hol, W. G., Drenth, J. & Betzel, C. (1989) *J. Mol. Biol. 206*, 365.
Schultz, P. G., Au, K. G., & Walsh, C. T. (1985) *Biochemistry 24*, 6840.
Schulz, G. E., Schirmer, R. H., Sachsenheimer, W., & Pai, E. F. (1978) *Nature 273*, 120.
Schulz, G. E., Schirmer, R. H., & Pai, E. F. (1982) *J. Mol. Biol. 160*, 287.
Schiering, N., Stoll, V. S., Blanchard, J. S., & Pai, E. F. (1989) *J. Biol. Chem. 264*, 21144.
Stoll, V. S., & Blanchard, J. S. (1988) *Arch. Biochem. Biophys. 260*, 752.
Vanoni, M. A., Wong, K. K., Ballou, D. P., & Blanchard, J. S. (1990) *Biochemistry 29*, 5790.
Williams, C. H., Jr. (1976) *Enzymes* (Boyer, P. D., Ed.) Vol. XIII, pp 89-173, Academic Press, New York.
Wong, K. K. & Blanchard, J. S. (1989) *Biochemistry 28*, 3586.

Steady-State Redox Behavior of Cytochrome *c*, Cytochrome *a*, and Cu_A of Cytochrome *c* Oxidase in Intact Rat Liver Mitochondria†

Joel E. Morgan* and Mårten Wikström
Helsinki Bioenergetics Group, Department of Medical Chemistry, University of Helsinki, Siltavuorenpenger 10A, SF-00170 Helsinki, Finland

Received April 26, 1990; Revised Manuscript Received August 6, 1990

ABSTRACT: We have examined the steady-state redox behavior of cytochrome *c* (Fe_c), Fe_a, and Cu_A of cytochrome *c* oxidase during steady-state turnover in intact rat liver mitochondria under coupled and uncoupled conditions. Ascorbate was used as the reductant and TMPD (*N,N,N',N'*-tetramethyl-1,4-phenylenediamine) as the redox mediator. After elimination of spectroscopic interference from the oxidized form of TMPD, we found that Fe_a remains significantly more oxidized than previously thought. During coupled turnover, Cu_A always appears to be close to redox equilibrium with Fe_c. By increasing the amount of TMPD, both centers can be driven to fairly high levels of reduction while Fe_a remains relatively oxidized. The reduction level at Fe_a is close to a linear function of the enzyme turnover rate, but the levels at Fe_c and Cu_A do not keep pace with enzyme turnover. This behavior can be explained in terms of a redox equilibrium among Fe_c, Cu_A, and Fe_a, where Fe_a is the electron donor to the oxygen reduction site, but only if Fe_a has an effective E_m (redox midpoint potential) of 195 mV. This is too low to be accounted for on the basis of nonturnover measurements and the effects of the membrane potential. However, if there is no equilibrium, the internal $Cu_A \rightarrow Fe_a$ electron-transfer rate constant must be slow in the time average (about 200 s^{-1}). Other factors which might contribute to such a low E_m are discussed. In the presence of uncoupler, this situation changes dramatically. Both Fe_c and Cu_A are much less reduced; within the resolution of our measurements (about 10%), we were unable to measure any reduction of Cu_A. Fe_a and Cu_A remain too oxidized to be in redox equilibrium with Fe_c during steady-state turnover. Furthermore, our results indicate that, in the uncoupled system, the (time-averaged) internal electron-transfer rate constants in cytochrome oxidase must be of the order of 2500 s^{-1} or higher. When turnover is slowed by azide, the relative redox levels at Fe_a and Fe_c are much closer to those predicted from nonturnover measurements. In presence of uncouplers, Fe_a is always more reduced than Fe_c, but in the absence of uncouplers, the two centers track together. Unlike the uninhibited, coupled system, the redox behavior here is consistent with the known effect of the electrical membrane potential on electron distribution in the enzyme. Interestingly, in these circumstances (azide and uncoupler present), Fe_a behaves as if it were no longer the kinetically controlling electron donor to the bimetallic center.

Cytochrome *c* oxidase is a biological energy transducer. The enzyme couples a redox reaction, the reduction of dioxygen to water by cytochrome *c*, to the production of an electrochemical proton gradient across the inner mitochondrial membrane. There appear to be two separate processes of energy conservation involved. One is essentially part of the redox reaction itself: The oxidation of one molecule of dioxygen to water requires four electrons and four protons. The enzyme is arranged in such a way that the electrons come from cytochrome *c* on the outside of the membrane, while the

† This work has been supported by a research grant from the Sigrid Jusčlius Foundation. J.E.M. is the recipient of an Academy of Finland postdoctoral research fellowship.
* To whom correspondence should be addressed.

0006-2960/91/0430-948$02.50/0